

Real-Time Fluorimetric Analysis of Gramicidin D- and Alamethicin-Induced K^+ Efflux from Sf9 and Cf1 Insect Cells[†]

Gilles Guihard,^{‡,§} Saïd Falk,^{||} Vincent Vachon,^{||} Raynald Laprade,^{||} and Jean-Louis Schwartz^{*,‡,||}

Biotechnology Research Institute, National Research Council, 6100 Royalmount Avenue, Montreal, Quebec, H4P 2R2, and the Groupe de recherche en transport membranaire, Université de Montréal, Montreal, Quebec, H3C 3J7, Canada

Received January 20, 1999; Revised Manuscript Received March 19, 1999

ABSTRACT: Gramicidin D and alamethicin are pore-forming peptides which exhibit lethal properties against a large spectrum of cells. Despite a wealth of experimental data from artificial membranes, the time course and quantitative analysis of the activity of these ionophores are not well described in living cells. In the present study, the newly described fluorescent dye CD-222 was used to monitor extracellular potassium ion concentration and report the effects of these antibiotics on the K^+ permeability of the plasma membrane of *Spodoptera frugiperda* (Sf9) and *Choristoneura fumiferana* (Cf1) insect cells. Both peptides induced a rapid efflux of intracellular K^+ as a consequence of ion channel formation in the cell membrane. K^+ efflux began without any measurable delay. While the final extracellular K^+ concentration was unaffected by ionophore concentration, the rate of K^+ efflux was dose dependent. Using a model describing the partition of the peptides in lipid membranes, the K^+ efflux kinetic parameters were determined for both cell types and both pore formers. The proposed stoichiometry for the channel formed by gramicidin in living cells is in good agreement with the two-monomers model based on data from artificial membrane systems. The K^+ -permeable channel formed by alamethicin in insect cells appears to involve three monomers.

Ion segregation across biological membranes is critical for cell function and is responsible for numerous physiological processes such as nerve conduction, excitation-contraction, and excitation-secretion couplings. Several polypeptide antibiotics, including gramicidin D and alamethicin, are known to exert their lethal properties by permeabilizing the cell membrane, thus disrupting ionic gradients and abolishing secondary transport activities.

Gramicidin D from *Bacillus brevis* increases the ionic permeability of numerous biological membranes (1–3), including the cytoplasmic membrane of Gram-positive and Gram-negative bacteria (4, 5), the inner mitochondrial membrane (6) and the plasma membrane of erythrocytes (7–9), fibroblasts (10, 11), skeletal muscle cells (12–14), and immune cells (15–18). Gramicidin is a pentadecapeptide of alternating D- and L-amino acids organized as a $^{6.3}\beta$ -helix (see ref 19 for a review). Many of the features concerning the ionophoric effects of gramicidin have been inferred from experiments demonstrating its ability to form cation-selective channels in planar lipid bilayers and liposomes (20–24). A head-to-head dimer model describing the gramicidin channel

formed in artificial membranes has been abundantly documented (25–28).

Alamethicin, a 20-amino acid peptide secreted by the fungus *Trichoderma viride* (reviewed in ref 29) is also a membrane-permeabilizing agent (30–35). It inserts into lipid bilayers and forms cation-selective voltage-gated channels (36–39). Alamethicin is organized as an α -helix with a proline-induced kink in position 14 (40). It was proposed that the C-terminal part of the molecule adopts a β -strand conformation (41). Insertion of alamethicin into lipid bilayers occurs above a critical peptide:lipid ratio, while channel formation and/or opening require a transmembrane voltage and involve hydrogen-bond-triggered aggregation of alamethicin molecules (42–47). Hall et al. (48) have proposed that the alamethicin channel is composed of 2–11 monomers depending on the alkyl chain length of the lipid forming the bilayer. Nine monomers were considered by Stankowski and Schwarz (49). He et al. (50), on the basis of neutron scattering experiments, indicated that two channel forms may exist with 8–9 or 11 monomers per channel, respectively.

Despite a wealth of data obtained from experiments conducted on artificial membrane systems, there is little information on the properties of the channels formed by gramicidin and alamethicin in living cells, and the channel stoichiometry remains to be determined under these conditions. In the present study, CD-222,¹ a newly described

[†] This work was supported in part by Strategic Grant STR0167557 from the Natural Sciences and Engineering Research Council (NSERC) of Canada (to R.L. and J.L.S.).

* To whom all correspondence should be addressed. Phone: (514) 496-6355. Fax: (514) 496-6213. E-mail: jean-louis.schwartz@bri.nrc.ca. NRCC publication No: 41839.

[‡] National Research Council.

[§] Supported by a NSERC Visiting Fellowship in Canadian Government Laboratories. Present address: Laboratoire de physiologie et pharmacologie cellulaire et moléculaire, Hôpital Hôtel-Dieu, Bâtiment HNB, 44093 Nantes, France.

^{||} Université de Montréal.

¹ Abbreviations: CD-222, coumarin diacid cryptand [2'.2'.2'] (19²,24²-dioxo-4,7,13,16,20,23-hexaoxa-1,10-diaza-19(7,6),24(6,7)-di(2H-2-benzopyrana)bicyclo [8.8.6]tetracosaphane-19³,24³-dicarboxylic acid); Me₂-SO, dimethyl sulfoxide; Pipes, 1,4-piperazinediethanesulfonic acid; SEM, standard error of the mean.

potassium-sensitive fluorescent dye (51), was used to monitor the time course of the K⁺ efflux resulting from the exposure of lepidopteran insect cells (Sf9, from *Spodoptera frugiperda*, and Cf1, from *Choristoneura fumiferana*) to gramicidin D and alamethicin. Both peptides dramatically increased the cells' plasma membrane permeability to K⁺ and induced the complete depletion of intracellular K⁺. The K⁺ efflux proceeded without delay and with a rate that was clearly related to peptide concentration. A mathematical model describing ionophore partition into the plasma membrane was developed to determine channel stoichiometry. It is concluded that the pores formed by gramicidin D in living cells involve two monomers and that those formed by alamethicin involve three monomers.

EXPERIMENTAL PROCEDURES

Chemicals. Grace's insect cell culture medium (52) and Pluronic F-68 were obtained from Gibco BRL (Burlington, Ont.), and fetal bovine serum was from Hyclone (Logan, UT). CD-222 was purchased from Molecular Probes (Eugene, OR). It was dissolved in Me₂SO to a final concentration of 20 mM. Alamethicin and gramicidin D (a mixture containing 80% gramicidin A, 5% gramicidin B, and 15% gramicidin C) were obtained from Sigma, St. Louis, MO. They were solubilized in Me₂SO and stored at -20 °C until use. The ionophore solutions were briefly sonicated (30–60 s) before use. All other reagents were of analytical grade.

Cell Cultures. Sf9 (ATCC CRL 1711) and Cf1 cells were grown in Grace's medium supplemented with 10% (v/v) heat-inactivated fetal bovine serum and 0.1% (w/v) Pluronic F-68 at 27 °C. Cells were harvested during mid-logarithmic phase by centrifugation (180g, 20 min, room temperature). Pellets were resuspended at (100–120) × 10⁶ cells mL⁻¹ in simplified Grace's medium (53) from which KCl was omitted [G*Ko medium containing (mM): 21 NaCl, 14 MgCl₂, 11 MgSO₄, 6.8 CaCl₂, and 10 Pipes/Tris (pH 6.3)] or replaced by 50 mM *N*-methyl-D-glucamine hydrochloride (G*KoNMDG medium). The osmolarity of the media was adjusted to 380 mosmol kg⁻¹ H₂O with sucrose. Under these conditions, viability of the cells was 96% as deduced from their ability to exclude trypan blue. Cells were used within 3 h following harvesting.

Protein Measurements. The protein content of Sf9 and Cf1 cells was 0.16 ± 0.02 (*n* = 6) and 0.19 ± 0.01 (*n* = 3) mg of protein per 10⁶ cells, respectively, as determined by the method of Bradford (54).

CD-222 Fluorescence Calibration. Emission spectra were recorded (λ_{ex} = 360 nm, 5-nm slits width) with a SPEX-FLUOROLOG CM-3 (JY/Spex Instruments SA, Edison, NJ) in a 1 cm optical path length cuvette filled with G*Ko medium and various CD-222 concentrations. The temperature was regulated at 27 °C. Calibration of the fluorescence signal as a function of [K⁺], the extracellular potassium concentration was performed at the beginning of each experimental session. Briefly, 12 × 10⁶ cells were washed in 50 mL of G*Ko medium and resuspended in 2 mL of G*Ko medium containing 5 μM CD-222. Emission spectra were recorded for various [K⁺] between 0 and 50 mM. The fluorescence intensity recorded at 470 nm (*F*⁴⁷⁰) was normalized as Δ*F*/*F* = (*F*⁴⁷⁰ - *F*_{min}⁴⁷⁰)/*F*_{min}⁴⁷⁰, where *F*_{min}⁴⁷⁰ is the fluorescence intensity determined in the absence of K⁺. Normalized

fluorescence intensity was plotted as a function of [K⁺] to determine the apparent affinity *K*_d of CD-222 for [K⁺] and *F*_{max}⁴⁷⁰ using the equation below:

$$\Delta F/F = F_{\max}^{470} [K^+]/(K_d + [K^+]) \quad (1)$$

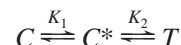
The effect of sodium on CD-222 fluorescence was tested as follows: 12 × 10⁶ cells were washed with 50 mL of G*Nao medium containing (mM) 21 KCl, 14 MgCl₂, 11 MgSO₄, 6.8 CaCl₂, and 10 Pipes/Tris (pH 6.3, 380 mosmol kg⁻¹ H₂O) and resuspended in 2 mL of G*Nao with 5 μM CD-222. Emission spectra were recorded for various [Na⁺] between 0 and 50 mM. Normalized *F*⁴⁷⁰ [i.e., (*F*_[Na⁺]⁴⁷⁰ - *F*_[0 Na⁺]⁴⁷⁰)/*F*_[0 Na⁺]⁴⁷⁰] was expressed as a function of [Na⁺].

Monitoring External [K⁺]. Insect cells were incubated (6 × 10⁶ cells mL⁻¹) in G*Ko medium with 5 μM CD-222 under continuous stirring. Gramicidin D or alamethicin were added to the cells and the variation of CD-222 *F*⁴⁷⁰ was recorded. The variation of [K⁺] was deduced from that of *F*⁴⁷⁰ using the following equation (55):

$$[K^+] = K_d (F^{470} - F_{\min}^{470}) / (F_{\max}^{470} - F^{470}) \quad (2)$$

It was verified that 0.5% (v/v) Me₂SO did not affect the permeability of Sf9 and Cf1 cells to K⁺.

K⁺ Efflux Analysis. The K⁺ efflux was modeled using the following scheme for the insertion of gramicidin D or alamethicin into the cell membrane:



where *C* and *C*^{*} are the concentrations of monomeric peptide in the bulk phase and in the cell membrane, respectively, *T* is the concentration of functional channels made of *n* aggregated monomers, and *K*₁ and *K*₂ are kinetic constants. It was assumed that, similarly to the situation observed in artificial membranes, *C*^{*} and *T* are also in equilibrium in biological membranes, which implies that the process of aggregation is fast compared to that of insertion into the membrane which involves diffusion of the monomers in the aqueous phase followed by their partitioning across the aqueous phase–membrane interface (27, 56, 57).

Therefore,

$$T = K_2 (C^*)^n \quad (3)$$

The kinetics of peptide insertion into the cell membrane can be described by a single exponential (56, 58):

$$C^* = C_{\infty}^* [1 - \exp(-t/\tau)] \quad (4)$$

where *C*_∞^{*} is the ionophore concentration in the membrane at equilibrium and τ is the apparent time constant of its insertion into the membrane. *C*_∞^{*} is related to *C* by

$$C_{\infty}^* = K_1 C \quad (5)$$

Therefore, from eqs 3, 4, and 5,

$$T = (K_1)^n K_2 C^n [1 - \exp(-t/\tau)]^n \quad (6)$$

The rate of change of intracellular K⁺ concentration [K⁺_{in}] after peptide addition is given by

$$d[K^+]_{in}/dt = -\alpha T[K^+]_{in} \quad (7)$$

where $[K^+]_{in}$ is the intracellular K^+ concentration and α is a constant that depends on the properties of the lipid bilayer.

$[K^+]_{out}$, the extracellular K^+ concentration, is related to $[K^+]_{in}$ by

$$[K^+]_{out}V_{out} + [K^+]_{in}V_{in} = \delta \quad (8)$$

where δ is a constant and V_{in} and V_{out} are the volumes of the intracellular and extracellular compartments, respectively. Therefore, VK^+ , the rate of change of $[K^+]_{out}$, is given by

$$VK^+ = d[K^+]_{out}/dt = \alpha T(V_{in}/V_{out})[K^+]_{in} \quad (9)$$

Thus, from eq 6,

$$VK^+ = \alpha(K_1)^n K_2 (V_{in}/V_{out}) [K^+]_{in} C^n [1 - \exp(-t/\tau)]^n \quad (10)$$

According to eq 10, VK^+ is a function of ionophore concentration, channel stoichiometry, and the time constant of the ionophore interaction with the membrane.

Using eq 6, the solution of eq 7 is given by

$$[K^+]_{in} = \lambda \exp(-AC^n I_n) \quad (11)$$

where $A = \alpha(K_1)^n K_2$, λ is an integration constant that is obtained at $t = 0$ when $[K^+]_{in}$ is maximum and I_n is given by

$$I_n = \int [1 - \exp(-t/\tau)]^n dt \quad (12)$$

For any n , the solution of eq 12 is

$$I_n = t + \tau \sum_{p=1}^{p=n} \frac{(-1)^{p+1}}{p} \frac{n!}{p!(n-p)!} \exp(-pt/\tau) \quad (13)$$

At the inflection points of the K^+ efflux curves, i.e., at time t_1 when $VK^+ = VK^+_{1/2}$ and $dVK^+/dt = 0$, combining eqs 11 and 13 provides

$$\frac{d^2 I_n}{dt^2} = AC^n \left(\frac{dI_n}{dt} \right)^2 \quad (14)$$

Let $X = \exp(-t/\tau)$. For any ionophore concentration C and at the corresponding t_1 , eq 14 becomes

$$\frac{nX}{(1-X)^{n+1}} = AC^n \tau \quad (15)$$

Therefore, for any pair of ionophore concentrations (C_p , C_{p+1}) and at the corresponding t_1 times, the following recurrence relation is obtained:

$$\left(\frac{X_{p+1}}{X_p} \right) \left(\frac{1-X_p}{1-X_{p+1}} \right)^{n+1} = \left(\frac{C_{p+1}}{C_p} \right)^n \quad (16)$$

from which the values of n and τ were calculated. To do so, experimental data were derived from each K^+ efflux curve that was fitted by a fifth order polynomial function ($R^2 > 0.990$) to obtain the precise coordinates of the inflection point where the second derivative of the polynomial function was equal to zero.

Alternatively, $VK^+_{1/2}$ was plotted against ionophore concentration. Data were fitted by the following Hill-like equation:

$$VK^+_{1/2} = \frac{VK^+_{max} C^c}{(EC_{50})^c + C^c} \quad (17)$$

where C is the ionophore concentration, VK^+_{max} the maximal rate of K^+ efflux, EC_{50} the ionophore concentration at which $VK^+_{1/2}$ is half-maximal and c the Hill coefficient of the process.

Data analysis and curve fitting were performed on a personal computer using SigmaPlot (version 5.0, Jandel Scientific Corporation, San Rafael, CA) and Mathematica (59) softwares.

RESULTS

CD-222 Fluorescence Calibration. The relationship between CD-222 concentration and fluorescence intensity was first determined from experimental data obtained in the absence of cells (Figure 1A). Experiments were performed at 27 °C, the temperature used for cell culture. Emission spectra were recorded (Figure 1A, inset) for different concentrations of CD-222 in G*Ko medium. The spectra displayed a fluorescence peak at 470 nm, the amplitude of which was related to the fluorophore concentration. No spectral shift was observed as CD-222 concentration was increased (data not shown). Fluorescence intensity measured at 470 nm leveled off at concentrations above 30 μ M. A dose of 5 μ M CD-222 provided half of the maximal signal.

The CD-222 fluorescence signal was calibrated with Sf9 cells bathed in G*Ko medium to which various amounts of KCl were added (Figure 1B). The presence of cells did not affect the fluorescence peak wavelength. Fluorescence increased by 22% due to autofluorescence of the cells as determined in the absence of the probe (data not shown). The F^{470}_{min} intensity with Sf9 cells, but no added K^+ , was taken as F^{470}_{min} . When K^+ was added to the medium, $\Delta F/F$, the normalized fluorescence intensity at 470 nm, increased as a function of $[K^+]$ with a K_d of 20.88 mM and a F^{470}_{max} of $2.31 \times F^{470}_{min}$. These values compared well with those given for cell-free CD-222 calibration (60). Similar results were obtained with Cf1 cells (data not shown). Fluorescence intensity was measured with Sf9 cells bathed in media containing 21 mM KCl and various concentrations of Na^+ (Figure 1B, inset). Increasing $[Na^+]$ from 0 to 20 mM resulted in a $26 \pm 3\%$ ($n = 3$) reduction in fluorescence intensity, in agreement with previous observations showing that Na^+ decreases the affinity of CD-222 for K^+ (51).

Gramicidin D- and Alamethicin-Induced K^+ Efflux from Insect Cells. At the beginning of the CD-222 experiments on Sf9 cells and under control conditions, residual K^+ was detected in the incubation medium (Figure 2). This residual K^+ could be eliminated by further washing the cells in G*Ko medium (data not shown) at the expense of reduced viability (from 96 to 60%). Therefore, the experiments were conducted with no further washing. Figure 2 shows that, under control conditions, $[K^+]$ increased at the rate of $0.075 \pm 0.014 \mu$ mol $min^{-1} mg^{-1}$ protein ($n = 5$). The same basal K^+ permeability was observed when the cells were resuspended in G*KoNMDG medium (data not shown), ruling out a possible

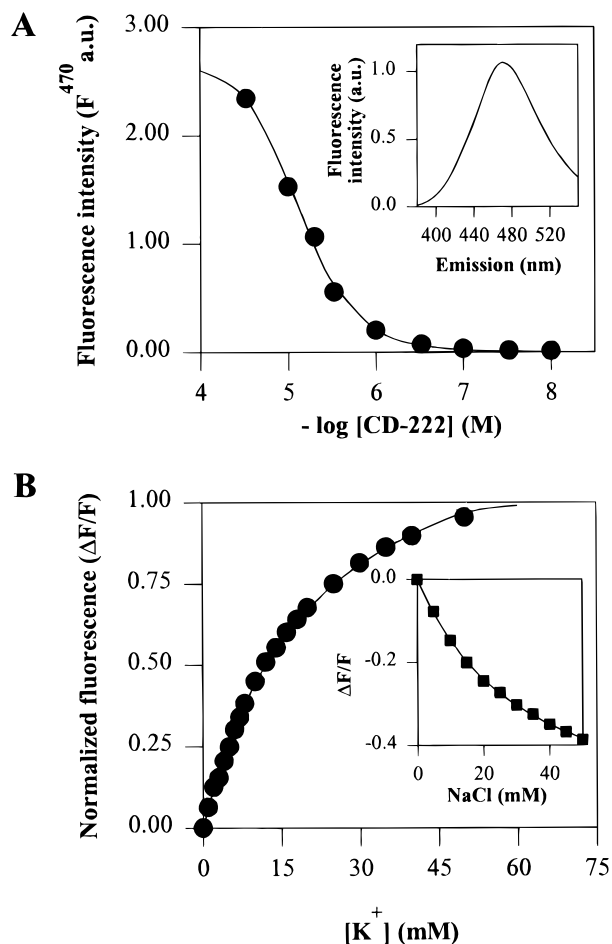


FIGURE 1: CD-222 fluorescence properties. (A) Fluorescence intensity (arbitrary units, a.u.) measured at $\lambda_{\text{em}} = 470$ nm (F^{470}) from emission spectra recorded between 380 and 550 nm as described in the Experimental Procedures, was plotted as a function of CD-222 concentration and fitted by a Hill-like equation (solid line, $R^2 = 0.997$). Data points are means of three independent experiments. Error bars are smaller than the symbols. (Inset) CD-222 (5 μM) emission spectrum in G*Ko medium. (B) Freshly harvested Sf9 cells were washed in G*Ko medium and resuspended in G*Ko medium containing 5 μM CD-222. Emission spectra were recorded as in panel A for each $[\text{K}^+]$ between 0 and 50 mM. F^{470} was measured after each KCl addition and normalized ($\Delta F/F$) as indicated in the Experimental Procedures. Data were fitted (solid line, $R^2 = 0.999$) for K_d and F_{max}^{470} determination using eq 1 in the Experimental Procedures. (Inset) Quenching of K⁺-dependent CD-222 fluorescence by Na⁺. CD-222 (5 μM) emission spectra were recorded in the presence of Sf9 cells resuspended in G*Nao medium ($[\text{K}^+] = 21$ mM). $[\text{Na}^+]$ was increased stepwise from 0 to 50 mM. In both graphs, data points are means of three independent experiments with error bars being smaller than the symbols.

alteration of the cells' K⁺ transport capacity due to reduced ionic strength. Furthermore, the basal permeability to K⁺ was also observed when the cells were incubated in the presence of 5 mM glucose or trehalose (data not shown), indicating that an unfavorable energetic state of the cells was not responsible for this K⁺ efflux. In contrast, no K⁺ efflux was observed in Cf1 cells even over a period of 10 min (not shown). These different behaviors may reflect different mechanisms of intracellular K⁺ homeostasis in the two cell lines.

Upon gramicidin D or alamethicin treatment of Sf9 cells, the extracellular $[\text{K}^+]$ increased to the same steady-state level. However, it was reached at different times depending on

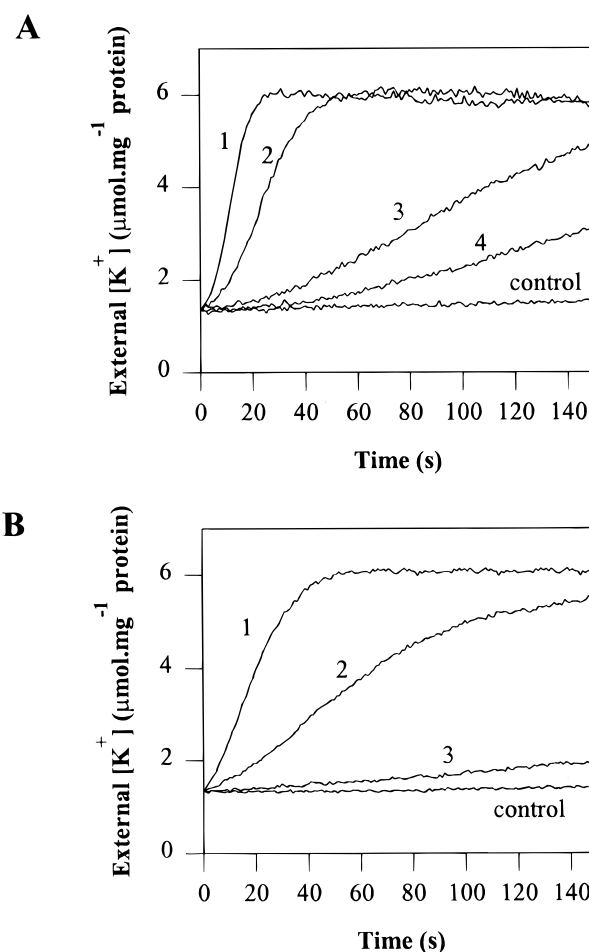


FIGURE 2: K⁺ efflux induced by gramicidin D and alamethicin from Sf9 cells. Freshly harvested Sf9 cells (6×10^6 cells mL^{-1}) were incubated in G*Ko medium containing 5 μM CD-222. (A) K⁺ efflux induced by the addition (at $t = 0$) of 1, 0.3, 0.1, and 0.03 $\mu\text{g} \cdot \text{mL}^{-1}$ gramicidin D (traces 1, 2, 3, and 4). (B) K⁺ efflux induced by the addition (at $t = 0$) of 3, 2, and 1 $\mu\text{g} \cdot \text{mL}^{-1}$ alamethicin (traces 1, 2, and 3). The control traces correspond to the variation of extracellular $[\text{K}^+]$ observed in the absence of the ionophores and with or without 0.5% Me₂SO. Each trace is representative of three independent experiments.

ionophore dose (Figure 2). The total amount of K⁺ released into the medium, i.e., the steady-state $[\text{K}^+]$ less the initial $[\text{K}^+]$, was $4.43 \pm 0.17 \mu\text{mol} \cdot \text{mg}^{-1}$ protein ($n = 24$) for Sf9 cells. Similar K⁺ effluxes were recorded from Cf1 cells treated with gramicidin D or alamethicin (data not shown). The total amount of K⁺ released from Cf1 cells was $3.93 \pm 0.13 \mu\text{mol} \cdot \text{mg}^{-1}$ protein ($n = 24$). No delay was detectable in the K⁺ efflux induced by gramicidin D or alamethicin from Sf9 cells (Figure 2) or Cf1 cells (data not shown). The time-course of the K⁺ efflux induced by gramicidin D or alamethicin from Sf9 (Figure 2) and Cf1 cells (not shown) exhibited a sigmoidal shape. The time at which VK^+_1 was determined depended on peptide concentration (Figure 2), but the amount of intracellular K⁺ released from each cell type by each ionophore was the same at all the times at which VK^+_1 was obtained. Therefore, $[\text{K}^+]_{\text{in}}$ was a constant parameter in eq 10.

Kinetic Analysis of K⁺ Efflux from Insect Cells Induced by Gramicidin D and Alamethicin. Channel formation by gramicidin D or alamethicin in the plasma membrane of Sf9 and Cf1 cells was described by the model given in the

Table 1: Kinetic Parameters of Gramicidin D- and Alamethicin-induced K^+ Efflux

	gramicidin D		alamethicin	
	Sf9	Cf1	Sf9	Cf1
kinetic model				
n	1.73 ± 0.07	2.10 ± 0.08	2.74 ± 0.02	3.01 ± 0.06
τ (s)	98 ± 13	114 ± 13	142 ± 6	115 ± 8
Hill-like analysis				
VK^+_{max} ($\mu\text{mol min}^{-1} \text{mg}^{-1} \text{protein}$)	19.46	29.01	48.34	34.33
EC_{50} ($\mu\text{g mL}^{-1}$)	0.410	0.303	4.74	4.41
Hill coefficient c	1.65	1.55	3.15	3.37

Experimental Procedures. Using the fact that $[K^+_{in}]$ is a constant at VK^+_I (see above), eq 16 was used to determine the stoichiometry n of the channels formed by gramicidin D and alamethicin and to estimate the apparent time constant τ of their insertion into the cell membrane. Using the ionophore concentration, the resulting VK^+_I and the corresponding time t_I at which VK^+_I was determined, n and τ were calculated for gramicidin D and alamethicin in Sf9 and Cf1 cells (Table 1).

Alternatively, VK^+_I was plotted against ionophore concentration, displaying a saturation process for both peptides (Figure 3). Therefore, a Hill-like plot analysis (eq 17 in the Experimental Procedures) was performed. The resulting values for VK^+_{max} , EC_{50} , and c , the Hill coefficient, are given in Table 1.

DISCUSSION

The channel properties of gramicidin D and alamethicin have been extensively studied in artificial membrane systems (21, 25, 26, 42, 48, 50). While the permeabilizing effect of gramicidin on living cells has been qualitatively described, there is no such data concerning alamethicin. The present work is the first quantitative study of the ionophoric effects of these two peptides on living cells of insects. It clearly shows that both peptides induce a significant increase in the membrane permeability to K^+ in Sf9 and Cf1 cells. K^+ efflux occurred with no delay and proceeded at a rate that was strongly related to ionophore concentration.

Redistribution of ionic gradients following exposure of cells and organelles to different ionophoric antibiotics has been characterized by different means including ion-specific electrodes, radioisotope flux measurements, and biochemical assays (61–64). Similar observations using intracellular Ca^{2+} -, K^+ -, and pH-sensitive fluorescent dyes have also been reported for insect cells exposed to *Bacillus thuringiensis* toxins (65–67). In the present study, a quantitative assay based on the spectroscopic properties of CD-222 used as an extracellular K^+ probe has been developed to monitor the time course of the efflux of this ion from living cells treated with gramicidin D and alamethicin. Extracellular K^+ dye allows easy signal calibration and thus precise quantitative measurements. Moreover, the fluorescent signal is not altered by sequestration into intracellular compartments. Our results demonstrate that when Sf9 and Cf1 cells were incubated in a simplified physiological solution containing CD-222, the fluorescence intensity of the probe was related to $[K^+]$ with an apparent K_d of 20.88 mM. K^+ -dependent CD-222 fluorescence variations were influenced by the presence of Na^+ as reported for the K^+ -sensitive dye PBFI (68). Although this may represent a complicating factor for studies on

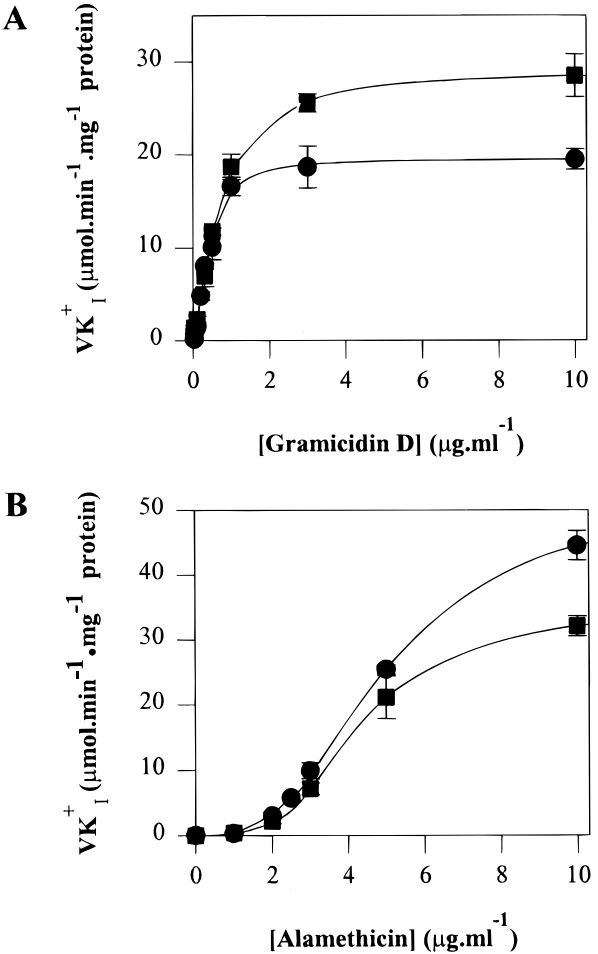


FIGURE 3: Hill-like plot analysis of the K^+ efflux induced by gramicidin D and alamethicin. VK^+_I was determined for each efflux curve from Sf9 (●) and Cf1 (■) cells as described in the Experimental Procedures and corrected by subtracting the rate of K^+ efflux observed under control conditions. Plots of VK^+_I vs gramicidin D (A) or alamethicin (B) concentrations were constructed and the points were fitted using eq 17 in the Experimental Procedures (A, $R^2 = 0.992$ for Sf9 and 0.994 for Cf1 cells; B, $R^2 = 0.999$ for both cell types). Values are means \pm SEM for three independent experiments.

mammalian cells, the CD-222 technique proves very useful for insect cells that can best be grown in low Na^+ -containing media (52).

Quantification of extracellular K^+ concentration at the end of the K^+ efflux supports the fact that both alamethicin and gramicidin D induce the complete depletion of intracellular K^+ from Sf9 and Cf1 cells. The mechanism responsible for neutralization of K^+ electrical charges remains to be clarified in these cells. It may be accomplished by external cations flowing through the peptide-made channels or by intracellular

anions flowing through endogenous chloride channels such as those previously described in Sf9 cells (66). The sigmoidal shape of the K⁺ efflux curves suggests that, following addition of ionophore to the cells, an increasing number of de novo K⁺-conducting channels are recruited in the cell membrane and that the subsequent progressive drop in K⁺ efflux rate is due to the collapse of the K⁺ electrochemical gradient rather than a decrease in ionophore activity, as described by Mak and Webb (69) who observed short-lived (≤ 1 min) alamethicin channels in artificial lipid bilayers.

In living cells, the kinetic parameters of ion fluxes induced by gramicidin D or alamethicin have never been determined, and so far, there was no data on the stoichiometry of these channels. Under the conditions of the present study, the K⁺ efflux from peptide-treated Sf9 and Cf1 cells did not display any detectable delay and kept increasing until the inflection point was attained. This suggests that gramicidin D and alamethicin interact directly with the cell membrane following a single-exponential process in a manner similar to that observed in artificial lipid bilayers (20, 37, 58). Our analysis was based on the assumption that the two peptides are predominantly in monomeric form in the bulk phase and that they insert into the biological membranes as monomers. The monomeric state in solution has been largely discussed for gramicidin (70) and for alamethicin at low concentrations, i.e., within the concentration range used in this study (58, 71, 72). In an earlier study in which a model was proposed for the gramicidin channel reconstituted in azolectin liposomes, the ion fluxes through the channels were analyzed following a long period of preincubation of the liposomes with the ionophore (73). Our approach considers the kinetics of peptide integration into the cell membrane at a far earlier stage. In the kinetic model proposed in this study, we considered that the ionophores integrate into cell membranes of unlimited surface area and that no other restricting factors were present. This explains why the model does not predict saturation (see eq 10). Nevertheless, the model remains valid until $t = t_1$ when the K⁺ efflux curves reach their inflection points. Under these conditions, the model (eq 16 in which VK^+_1 and t_1 are determined for each peptide concentration) provided good estimates of τ , the time constant for ionophore integration, a parameter that has never been determined in living cells. The τ values found for both ionophores were similar in the two cells types, suggesting a similar integration process for both peptides. They are comparable to those found for the integration of macrotetrolide ionophores (57), confirming our hypothesis that the process of integration is slower than that of aggregation (58).

The stoichiometry of the channels formed by gramicidin and alamethicin in living cells, as provided by our model, is close to two for gramicidin D and three for alamethicin, suggesting that gramicidin forms a dimeric channel in the plasma membrane of living cells, while that of alamethicin is trimeric. For gramicidin, this is in good agreement with the data from liposome and planar lipid bilayer experiments (20–24, 27, 28, 73) and with the model proposed by Urry et al. (26). For alamethicin, the stoichiometry of the K⁺-conducting channels is still being debated. On one hand, a trimeric structural unit has been proposed by Fox and Richards (40) based on crystallographic data. On the other hand, the results of planar lipid bilayer, electron paramagnetic resonance, and more recently, neutron scattering experiments

have suggested that the alamethicin channel stoichiometry lies between 2 and 11 (48–50, 74). This wide range may be related to the fact that the apparent alamethicin stoichiometry can be affected by the lipid composition of the bilayer (48). Our results indicate that in insect cells, the alamethicin channel responsible for K⁺ efflux may result from the aggregation of three monomers following their insertion into the membrane. However, it cannot be excluded that the alamethicin pore assumes a larger stoichiometry long after intracellular K⁺ depletion has been completed.

The relationship between VK^+_1 and ionophore concentration displayed a saturable pattern. Therefore a Hill-like analysis was used to characterize this relationship. Interestingly, the Hill coefficients are close to the values for the stoichiometry calculated with eq 16 of the model derived for the gramicidin D and alamethicin channels. It appears therefore that under our conditions a Hill-like analysis can be used as a quantitative tool to describe the ionophoric properties of gramicidin and alamethicin in living cells, even if the transport mechanism may involve more than a single process at the molecular level. Saturation of VK^+_1 (i.e., the Hill VK^+_{max} parameter) may result from an upper limit to the number of gramicidin or alamethicin channels that can be formed in the cell membrane, or from limited membrane permeability to counterions. The difference in saturating rates observed in Sf9 and Cf1 cells may correspond to a difference in the maximal number of channels formed by each peptide. However, other factors, including differences in the lipid composition of the plasma membranes of Sf9 and Cf1 cells or in peptide-lipid interactions, may also be involved. Indeed, the rate of ionic diffusion through gramicidin D and alamethicin channels is affected by the lipid composition of the membrane (24, 34, 48).

In conclusion, this study shows, for the first time, that by using the K⁺-sensitive fluorescent dye CD-222 to monitor the time course of gramicidin D- and alamethicin-induced K⁺ efflux from living cells, a quantitative analysis of the ionophoric effects of these pore-forming peptides can be performed which provides new insight into their properties at the cellular level.

ACKNOWLEDGMENT

We thank Joanne Vallée (Groupe de recherche en transport membranaire, GRTM) and Léna Potvin (Biotechnology Research Institute, BRI) for their expert technical assistance, Robert Ménard (BRI) for providing access to his SPEX fluorimeter in the early phase of this work, and Alfred Berteloot (GRTM), Roland Brousseau (BRI), Luke Masson (BRI) and Olivier Peyronnet (GRTM) for helpful and stimulating discussions. We are indebted to Sardar Sohi (Canadian Forest Service, Natural Resources Canada, Sault Ste. Marie, Ontario) for the generous gift of Cf1 cells.

REFERENCES

1. Harris, E. J., and Pressman, B. C. (1967) *Nature* 216, 918–920.
2. Silman, H. I., and Karlin, A. (1968) *Proc. Natl. Acad. Sci. U.S.A.* 61, 674–679.
3. Podleski, T., and Changeux, J.-P. (1969) *Nature* 221, 541–545.
4. Katsu, T., Kobayashi, H., and Fujita, Y. (1986) *Biochim. Biophys. Acta* 860, 608–619.

5. Katsu, T., Kobayashi, H., Hirota, T., Fujita, Y., Sato, K., and Ngai, U. (1987) *Biochim. Biophys. Acta* 899, 159–170.
6. Luvisetto, S., and Azzone, G. F. (1989) *Biochemistry* 28, 1109–1116.
7. Otten-Kuipers, M. A., Beuner, T. L., Kronenburg, N. A., Roelofsen, B., and Op den Kamp, J. A. (1993) *Mol. Membr. Biol.* 13, 225–237.
8. Freedman, J. C., Novak, T. S., Bisognano, J. D., and Pratap, P. R. (1994) *J. Gen. Physiol.* 104, 961–983.
9. Ogino, T., Shulman, G. I., Avison, M. J., Gullans, S. R., den Hollander, J. A., and Shulman, R. G. (1985) *Proc. Natl. Acad. Sci. U.S.A.* 82, 1099–1103.
10. Friedberg, I., Weisman, G. A., and De, B. K. (1985) *J. Membr. Biol.* 83, 251–259.
11. Mastrocola, T., Flamigni, A., and Rugulo, M. (1991) *Biochim. Biophys. Acta* 1069, 201–208.
12. Caffier, G., and Shvinka, N. E. (1985) *Acta Biol. Med. Ger.* 38, 135–137.
13. Shvinka, N. E., and Toropova, F. V. (1985) *Gen. Physiol. Biophys.* 4, 493–500.
14. Caffier, G., and Shvinka, N. E. (1989) *Biomed. Biochim. Acta* 48, S552–S557.
15. Sarkadi, B., Mack, E., and Rothstein, A. (1984) *J. Gen. Physiol.* 83, 513–527.
16. Gamalei, I. A., Kaulin, A. B., and Kirpichnikova, K. M. (1991) *Tsitologia* 33, 60–66.
17. Beauvais, F., Shimahara, T., Inoue, I., Hieblot, C., Burtin, C., and Benveniste, J. (1992) *J. Immunol.* 148, 149–154.
18. Walev, I., Reske, K., Palmer, M., Valeva, A., and Bhakdi, S. (1995) *EMBO J.* 14, 1607–1614.
19. Koeppe, R. E., II, and Anderson, O. S. (1996) *Annu. Rev. Biophys. Biomol. Struct.* 25, 231–258.
20. Hladky, S. B., and Haydon, D. A. (1972) *Biochim. Biophys. Acta* 274, 294–312.
21. Myers, V. B., and Haydon, D. A. (1972) *Biochim. Biophys. Acta* 274, 313–322.
22. Neher, E., Sandblom, J., and Eisenman, G. (1978) *J. Membr. Biol.* 40, 97–116.
23. Busath, D., and Szabo, G. (1981) *Nature* 294, 371–373.
24. Chen, X., and Gross, R. (1995) *Biochemistry* 34, 7356–7364.
25. Ketchum, R. R., Roux, B., and Cross, T. A. (1997) *Structure* 5, 1655–1669.
26. Urry, D. W., Goodall, M. C., Glickson, J. D., and Mayers, D. F. (1971) *Proc. Natl. Acad. Sci. U.S.A.* 68, 1907–1911.
27. Baño, M. C., Braco, L., and Abad, C. (1991) *Biochemistry* 30, 886–894.
28. Koeppe, R. E., II, Berg, J. M., Hodgson, K. O., and Stryer, L. (1979) *Nature* 279, 723–725.
29. Sansom, M. S. P. (1993) *Eur. J. Biophys.* 22, 105–124.
30. Jones, L. R., Maddock, S. W., and Besh, H. R., Jr. (1980) *J. Biol. Chem.* 255, 9971–9980.
31. Wille, B., Franz, B., and Jung, G. (1989) *Biochim. Biophys. Acta* 986, 47–60.
32. Xie, Z., Wang, Y., Ganjeizadeh, M., McGee, R., Jr., and Askari, A. (1989) *Anal. Biochem.* 183, 215–219.
33. Fonteriz, R. I., Lopez, M. G., Garcia-Sancho, J., and Garcia, A. G. (1991) *FEBS Lett.* 283, 89–92.
34. Ritov, V. B., Tverdislova, I. L., Avakyan, T. Y. U., Menshikova, E. V., Leikin, Y. U. N., Bratkovskaya, L. B., and Shimon, R. G. (1992) *Gen. Physiol. Biophys.* 11, 49–58.
35. Ritov, V. B., Murzakhnetova, M. K., Tverdislova, I. L., Menshikova, E. V., Butylin, A. A., Avakyan, T. Y. U., and Yakovenko, L. V. (1993) *Biochim. Biophys. Acta* 1148, 257–262.
36. Mueller, P., and Rudin, D. O. (1968) *Nature* 217, 713–719.
37. Gordon, L. G. M., and Haydon, D. A. (1972) *Biochim. Biophys. Acta* 255, 1014–1018.
38. Eisenberg, M., Hill, J. E., and Mead, C. A. (1973) *J. Membr. Biol.* 14, 143–176.
39. Boheim, G., and Kolb, H.-A. (1978) *J. Membr. Biol.* 38, 99–150.
40. Fox, R. O., and Richards, F. M. (1982) *Nature* 300, 325–330.
41. Banerjee, U., Tsui, F.-P., Balasubramanian, T. N., Marshall, G. R., and Chan, S. I. (1983) *J. Mol. Biol.* 165, 757–775.
42. He, K., Ludtke, S. J., Heller, W. T., and Huang, H. W. (1996) *Biophys. J.* 71, 2669–2679.
43. Barranger-Mathys, M., and Cafiso, D. S. (1994) *Biophys. J.* 67, 172–176.
44. Wooley, G. A., and Wallace, B. A. (1992) *J. Membr. Biol.* 129, 109–136.
45. Latorre, R., and Alvarez, O. (1981) *Physiol. Rev.* 61, 77–150.
46. Cafiso, D. S. (1994) *Annu. Rev. Biophys. Biomol. Struct.* 23, 141–165.
47. Molle, G., Dugast, J. Y., Spach, G., and Duclohier, H. (1996) *Biophys. J.* 70, 1669–1675.
48. Hall, J. E., Vodyanoy, I., Balasubramanian, T. M., and Marshall, G. R. (1984) *Biophys. J.* 45, 233–247.
49. Stankowski, S., and Schwarz, G. (1989) *FEBS Lett.* 250, 556–560.
50. He, K., Ludtke, S. J., Worcester, D. L., and Huang, H. W. (1996) *Biophys. J.* 70, 2659–2669.
51. Crossley, R., Goolamali, Z., and Sammes, P. G. (1994) *J. Chem. Soc., Perkin Trans. 2*, 1615–1623.
52. Grace, T. D. C. (1962) *Nature* 195, 788–789.
53. Vachon, V., Paradis, M. J., Marsolais, M., Schwartz, J. L., and Laprade, R. (1995) *Biochemistry* 34, 15157–15164.
54. Bradford, M. (1976) *Anal. Biochem.* 72, 248–254.
55. Jezek, P., Mahdi, F., and Garlid, K. D. (1990) *J. Biol. Chem.* 265, 10522–10526.
56. Schwarz, G., Gerke, H., Rizzo V., and Stankowski, S. (1987) *Biophys. J.* 52, 685–692.
57. Bamberg, E., and Läuger, P. (1973) *J. Membr. Biol.* 11, 177–194.
58. Laprade, R., Grenier, F., Pagé-Dansereau, M., and Dansereau, J. (1984) *Can. J. Biochem. Cell Biol.* 62, 738–751.
59. Wolfram, S. (1993) *Mathematica: A System for Doing Mathematics by Computer*, Addison-Wesley, New York.
60. Haugland, R. P. (1996) in *Handbook of Fluorescent Probes and Research Chemicals* (Spence, M. T. Z., Ed.) Molecular Probes, Eugene, OR.
61. Bourdineaud, J.-P., Boulanger, P., Lazdunski, C., and Letellier, L. (1990) *Proc. Natl. Acad. Sci. U.S.A.* 87, 1037–1041.
62. Guihard, G., Bénédicti, H., Besnard, M., and Letellier, L. (1993) *J. Biol. Chem.* 268, 17775–17780.
63. Menestrina, G., Moser, C., Pellet, S., and Welsh, R. (1994) *Toxicology* 87, 249–267.
64. Huntley, J. S., and Hall, A. C. (1996) *Biochim. Biophys. Acta* 1281, 220–226.
65. Vachon, V., Paradis, M. J., Marsolais, M., Schwartz, J. L., and Laprade, R. (1995) *J. Membr. Biol.* 148, 57–63.
66. Schwartz, J. L., Garneau, L., Masson, L., and Brousseau, R. (1991) *Biochim. Biophys. Acta* 1065, 250–260.
67. Potvin, L., Laprade, R., and Schwartz, J. L. (1998) *J. Exp. Biol.* 201, 1851–1858.
68. Minta, M., and Tsien, R. Y. (1989) *J. Biol. Chem.* 264, 19449–19457.
69. Mak, D. O., and Webb, W. W. (1995) *Biophys. J.* 69, 2323–2336.
70. Haydon, D. A., and Lhakdy, S. B. (1972) *Q. Rev. Biophys.* 5, 187–282.
71. Archer, S. J., Ellena, J. E., and Cafiso, D. S. (1991) *Biophys. J.* 60, 389–398.
72. Rizzo, V., Stankowski, S., and Schwarz, G. (1987) *Biochemistry* 26, 2751–2759.
73. Bruggeman E. P., and Kayalar C. (1986) *Proc. Natl. Acad. Sci. U.S.A.* 83, 4272–4276.
74. Archer, S. J., and Cafiso, D. S. (1987) *Biophys. J.* 60, 380–388.